The influence of hydrocarbon expulsion on carbon isotopic compositions of individual *n*-alkanes in pyrolysates of selected terrestrial kerogens

Yuhong Liao, Ansong Geng *, Yongqiang Xiong, Dehan Liu, Jialan Lu, Jinzhong Liu, Haizu Zhang, Xinhua Geng

The state Key Laboratory of Organic Geochemistry, Guangzhou Institute of Geochemistry, Chinese Academy of Sciences, P. O. Box 1131, Wushan, Guangzhou 510640, China

Abstract

Expulsion of petroleum from source rock is a complex part of the entire migration process. There exist fractional effects on chemical compositions in hydrocarbon expulsion. Does the carbon isotopic fractionation occur during expulsion and to what extent? Here the influence of hydrocarbon expulsion on carbon isotopic compositions of individual *n*-alkanes from pyrolysates of selected terrestrial kerogens from Tuha basin and Fushun, Liaoning Province of China has been experimentally studied. The pyrogeneration-expulsion experiments were carried out under semi-closed system. The carbon isotopic compositions of individual *n*-alkanes were measured by GC-IRMS. The main conclusions are as follows. First, there is carbon isotopic fractionation associated with hydrocarbon expulsion from Type III kerogens in Tuha Basin. There exist differences of carbon isotopic compositions between the unexpelled *n*-alkanes and expelled *n*-alkanes from Tuha desmocollinite and Tuha mudstone. Second, there is almost no carbon isotopic fractionation associated with hydrocarbon expulsion from Type II kerogens in Fushun and Liaohe Basin. Third, carbon isotopic fractionation in hydrocarbon expulsion should be considered in making oil-source correlation of Type III kerogens at least in the Tuha Basin. Further studies need to be carried out to determine whether this is true in other basins. Fourth, oil and source at different maturity levels cannot be correlated directly for Type III kerogens since the carbon isotopic compositions of expelled hydrocarbons at different temperatures are different. The expelled hydrocarbons are usually lighter (depleted in ^{13}C) than the hydrocarbons remaining in the source rock at the same maturity.
© 2004 Elsevier Ltd. All rights reserved.

1. Introduction

The Turpan-Hami (Tuha) Basin hosts one of the most important coal-sourced oil fields in China. It is lo-

cated in eastern Xinjiang Province, NW China (Fig. 1). Through 1995 eight oil discoveries were made in Jurassic strata of Tuha Basin. Previous studies (Huang et al., 1991; Hendrix et al., 1995; Sun et al., 2000) showed that the Lower and Middle Jurassic coal-bearing sequences are the possible main source rocks of petroleum in Tuha Basin. There are two types of potential source rocks in the Basin. One is coal measures from Lower Jurassic

---

* Corresponding author. Fax: +86-85290706.
E-mail addresses: liaoyh@gig.ac.cn (Y. Liao), asgeng@gzb.ac.cn (A. Geng).
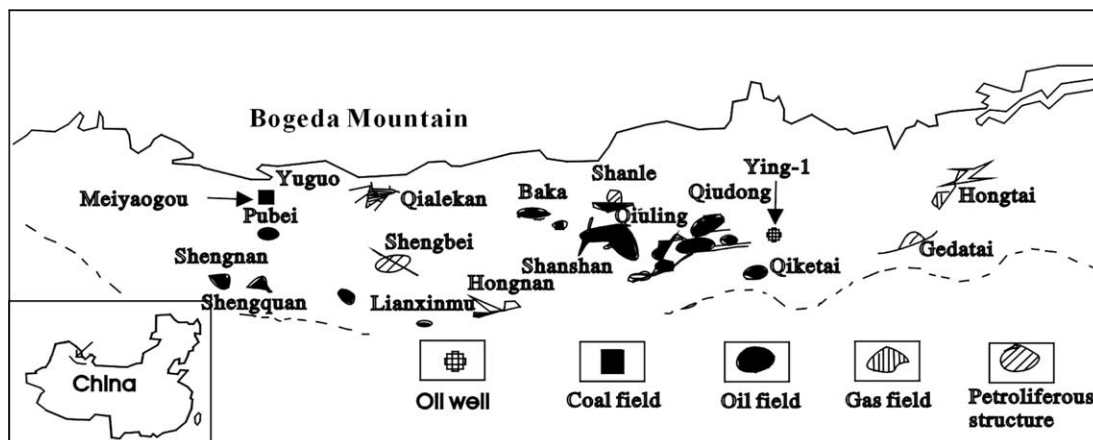
Fig. 1. The location of samples obtained in Turpan-Hami Basin: Meiyaogou coal mine and Ying-1 well.

Badaowan Formation and Middle Jurassic Xishanyao Formation, which are typical humic material (Type III). The other is Middle Jurassic mudstone of Qiketai Formation, which was deposited in a brackish lacustrine environment. The coal in Xishanyao Formation of Middle Jurassic (J_2x) is one of the main coal measures. There is also thick dark mudstone in this formation, which is a potential source rock.

Stable carbon isotopic compositions have been widely used in characterizing sources (Freeman et al., 1990; Hayes et al., 1990; Rieley et al., 1991), correlating oil with possible source rocks (Bjorøy et al., 1991, 1994; Karlsen et al., 1995; Stoddart et al., 1995) and reconstructing paleoenvironment and paleoclimate (Hayes et al., 1990; Schoell et al., 1994; Ruble et al., 1994). GC–IRMS has become a valuable technique for petroleum systems studies. GC–IRMS can be used to measure the isotopic value of specific compounds and thus it has furthered the studies of oil-source correlation.

Molecular geochemical methods have been used to correlate the oils and potential source rocks in Tuha Basin. Unfortunately, it was unsuccessful because the differences in the biomarkers among oils and source rocks are not big enough. Zhang (1997) compared the stable carbon isotopes of kerogen, total solvent extracts and bulk compound fractions for coals and interbedded shales from Jurassic coal measures in the Tuha Basin. The results showed that the difference of the carbon isotopic compositions between coals and shales is very small. Sun et al. (2000) also studied the isotopic compositions of individual *n*-alkanes of oil and source extracts (coals and interbedded shales in Turpan Basin). The study showed that alkanes of coal extracts are enriched in ^{13}C relative to those of interbedded shales. The carbon isotope excursions are in the range of 2–3‰.

The isotopic compositions of extracts from source rock and oil were analyzed in order to make a correlation of oil to possible source rock. The correlation of

oil to source rock is based on the assumption that the oil and the corresponding source rock have similar $\delta^{13}C$ values. In order to use isotopic compositions from crude oils and source rock extracts for oil/oil and oil/source correlations, two preconditions should be satisfied: the first is that the maturity of the oil and related source rock is similar; the second is that hydrocarbon expulsion has had no obvious effect on their isotopic composition (Xiong et al., 2003). However, there is large internal surface area in coal and the diameter of most pores within it is generally less than 5 Å (Van Krevelen, 1961). Therefore coal shows a strong capacity of adsorbing hydrocarbons generated in it. The expulsion of petroleum from shale is associated with chromatography-like fractionation effect according to the polarity of compounds (Leythaeuser et al., 1984). Coals have even stronger adsorptive capacity than shales, especially for those Type III coals with much desmocollinite in them. There is much evidence to suggest that the fractionation effect on chemical compositions is even larger in Type III kerogens than in Type II kerogens. Therefore there are some questions on stable carbon isotopic values associated with hydrocarbon expulsion as fractionation may have occurred and to some extent. This work focuses on these issues through thermal modelling.

2. Experiment

2.1. Samples

Three samples were chosen for this study: a desmocollinite (TH) and a dark mudstone (S38) from Tuha Basin, a cannel (ZM) from Fushun, NE of China. The desmocollinite (TOC = 71.88%, Ro = 0.5%) and the dark mudstone (TOC = 6.61%, Ro = 0.58%) are Type III kerogens. The cannel (TOC = 75.25%, Ro = 0.54%) is Type II oil prone kerogen (a kind of algal coal). The

desmocollinite and dark mudstone are both from the Middle Jurassic (J_2x), Xishanyao Formation. The former is from Meiyaogou coal mine and the latter is from Ying-1 well (Fig. 1).

2.2. Methods

The experimental system (Fig. 2) is similar to that of Geng et al. (1998). It is a semi-closed pyrolysis system. The dried coals and mudstone samples were powdered to 80 mesh and placed in the cylinder together with 40 g 60 mesh quartz as an underlayer. The underlying quartz also makes a distance for migration. Air was evacuated and the system was then heated. The generated gas and liquid pyrolysates can flow out of the cylinder freely into the tube and the gas volume measurer. The simulation temperatures for the Tuha desmocollite were 350, 380, 410 and 460 °C; for the mudstone 350, 380 and 410 °C; and for the Fushun sample 320, 350, 380, 410, 460 and 510 °C (Tables 1, 3, 5). In the experiment the cylinder was held isothermal and at a constant pressure (800 atm) for 72 h. At each temperature the heated sample and quartz were separately soxhlet ex-

tracted with chloroform. The light hydrocarbons expelled from the cylinder were collected in the tube (surrounded by cold traps) together with the heavy fractions. Hydrocarbons extracted from heated samples were defined as unexpelled hydrocarbons (EOM, extractable organic matter), and hydrocarbons collected in cold trap and extracted from quartz as expelled hydrocarbons. Asphaltene was precipitated by adding excess petroleum ether (b.p. 30–60 °C). The maltene fraction was separated into saturate, aromatic, and NSO polar fractions using column chromatography with petroleum ether, benzene and ethanol respectively. The saturate fraction was urea adducted to isolate the paraffin fraction containing only *n*-alkanes because simplified paraffin fractions allow for improved accuracy in isotope measurements without interference from co-eluting components or unresolved complex mixtures such as those comprising the background matrix. The method is similar to what was described by Ellis and Fincannon (1998). A saturated solution of urea in methanol was added to saturate fraction dissolved in a toluene-methanol solvent mixture. The urea mixture was left to stand overnight for complete adduction, then the solvent was

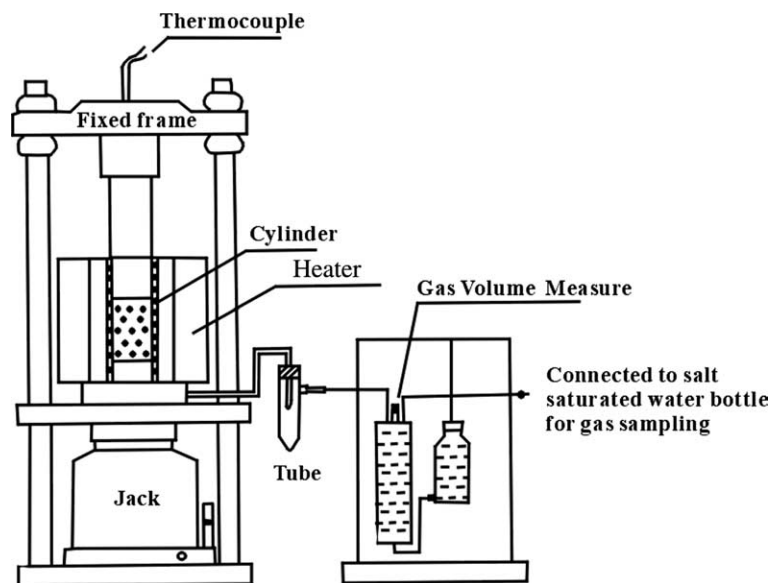Fig. 2. Diagram of the experimental pyrolysis system.

Table 1
Identifiers for *n*-alkanes (unexpelled and expelled) of TH at different temperatures

Temperature (°C):	350		380		410		460	
	EOM	Expelled	EOM	Expelled	EOM	Expelled	EOM	Expelled
	TH350C		TH380C	TH380L	TH410C	TH410L		TH460L
					TH410C*	TH410L*		

Table 2
$\delta^{13}C$ values (‰) for *n*-alkanes in pyrolysates (unexpelled and expelled) of Tuha desmocollinite at different temperatures

ID	THC	TH350C	TH380C	TH410C	TH380L	TH410L	TH460L	TH410C*	TH410L*
11							−25.1		−24.9
12						−23.9	−24.4	−23.9	−24.9
13	−27.4				−27.7	−24.1	−25.0	−23.7	−25.0
14	−26.9	−24.1			−29.9	−24.4	−24.2	−23.7	−24.9
15	−27.1	−24.9	−24.0		−28.3	−25.4	−25.1	−24.0	−25.3
16	−27.3	−25.1	−24.0	−23.4	−27.5	−25.4	−26.1	−24.6	−25.4
17	−26.8	−25.4	−24.3	−23.6	−27.5	−27.4	−25.4	−24.3	−25.8
18	−27.2	−24.9	−24.4	−23.7	−29.4	−27.3	−25.2	−25.0	−26.4
19	−27.8	−25.2	−24.7	−24.2	−28.4	−27.1	−24.9	−24.9	−26.2
20	−28.0	−25.0	−24.9	−24.0	−28.7	−26.8	−25.1	−25.0	−26.4
21	−28.2	−25.3	−24.5	−24.6	−27.9	−27.0	−25.7	−25.5	−26.5
22	−28.5	−25.5	−25.0	−24.2	−28.5	−27.3	−25.1	−25.1	−26.5
23	−28.6	−25.8	−25.2	−25.9	−27.1	−27.3	−25.8	−25.2	−26.6
24	−28.5	−26.9	−26.7	−25.4	−29.7	−26.8	−26.1	−24.7	−26.3
25	−28.4	−27.4	−27.2	−25.8	−30.0	−27.1	−25.4		−26.4
26	−28.3		−26.6	−25.5	−31.6	−27.4	−26.1		
27	−27.4		−26.6	−25.3	−31.1	−27.6	−25.7		
28	−27.3		−26.7	−26.3	−31.8	−27.8	−27.1		
29	−27.0		−27.3		−31.8	−27.8	−26.8		

ID, carbon number of *n*-alkanes.

Table 3
Identifiers for *n*-alkanes (unexpelled and expelled) of S38 at different temperatures

Temperature (°C):	350		380		410	
	EOM	Expelled	EOM	Expelled	EOM	Expelled
	S38-350C	S38-350L	S38-380C	S38-380L	S38-410C	S38-410L

pipetted from the urea precipitates. The urea precipitates were dried and then repeatedly rinsed with solvent to ensure complete removal of the non-adducted fractions. The *n*-alkanes were recovered with the addition of pentane or hexane after dissolution of the urea crystals in water. Then the *n*-alkanes were analyzed by GC and GC–C–IRMS.

2.2.1. Gas chromatography

The hydrocarbons were analyzed with a HP 6890 II GC equipped with a 50 m × 0.25 mm silica capillary column. The temperature program for the extracted hydrocarbons was from 80 °C (for 2 min) and then increased to 160 °C at a rate of 6 °C/min, then increased at a rate of 3 °C/min to 290 °C (for 30 min). The temperature program for expelled hydrocarbons was from 35 °C (held for 5 min) and then increased to 290 °C at a rate of 4 °C/min. Nitrogen was used as carrier gas with a flow rate of 1.0 ml/min.

2.2.2. Gas chromatography–combustion–isotope ratio mass spectrometry

GC–C–IRMS analyses were performed on a Delta Plus XL GC–C–IRMS system. The accuracy of the instrument was tested daily before sample analysis by

analyzing a mixture of *n*-alkanes and isoprenoid alkanes with known $\delta^{13}C$ values. The reproducibility was typically within ±0.5‰. Carbon isotope ratios for individual alkanes were calculated using a CO_2 reference gas, which was automatically introduced into the IRMS at the beginning and end of each analysis (Fig. 3). The data are reported in per mil (‰) relative to the PDB standard (Tables 2, 4, and 6).

3. Results and discussion

3.1. Carbon isotopic composition of individual n-alkanes in pyrolysates of Tuha desmocollinite

More hydrocarbons were generated and expelled out of the samples at higher temperatures. At 460 °C the EOM of desmocollinite was too low to be determined by GC–C–IRMS. The EOM of dark mudstone was almost depleted at 410 °C but still could be determined by GC–C–IRMS. At 350 °C the expelled *n*-alkanes were too low to measure the isotopic compositions. EOMs in proportion to total generated organic matter become less as temperatures increased and the expulsion efficiency increased at higher temperatures (Fig. 4).
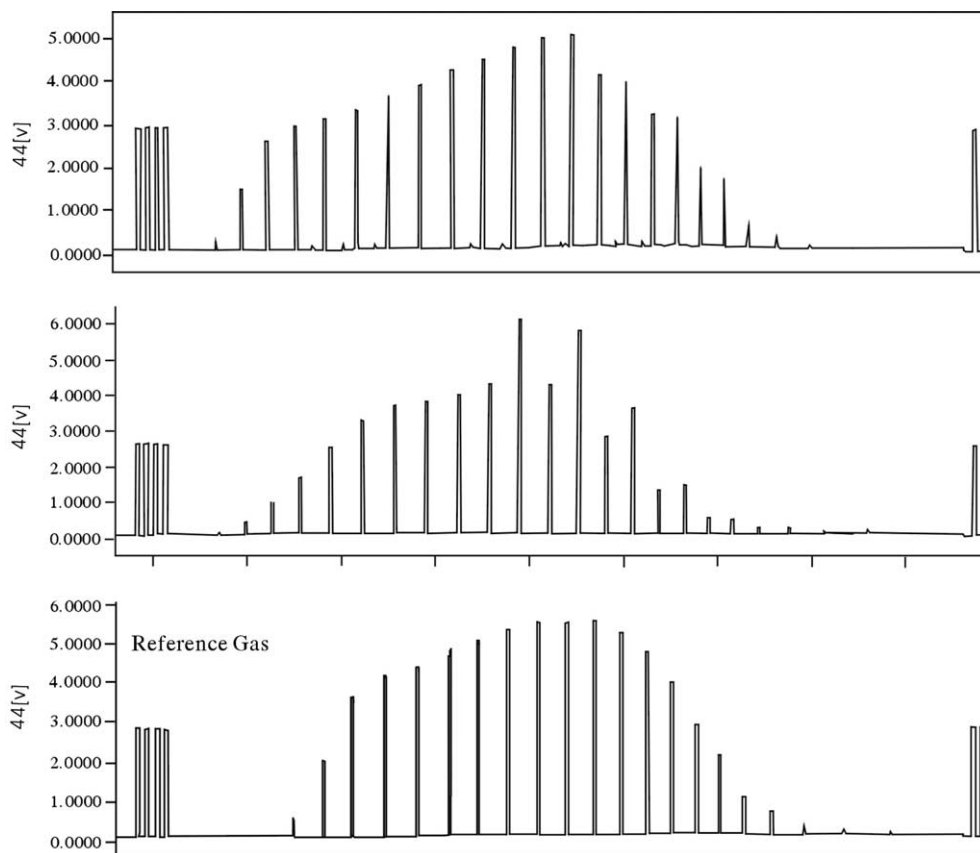
Fig. 3. Typical *m/z* 44 mass-chromatograms of unexpelled *n*-alkanes by GC–C–IRMS. Samples: ZM410C, TH350C, S38-350C.

Stable carbon isotopic compositions of *n*-alkanes from EOM were compared with those of the expelled hydrocarbons. The *n*-alkanes of unexpelled extracts become heavier as the temperature increases (Fig. 5(a)). THC identifies the original extracts from the desmocollinite. TH350C, TH380C, TH410C are unexpelled extracts from the desmocollinite at 350, 380 and 410 °C, respectively. The stable carbon isotopic compositions become heavier (rich in ^{13}C) at higher temperatures. The excursions of TH350C, TH380C and TH410C are in the range of 2‰. TH350C, TH380C and TH410C are all heavier than THC. TH410C is around 4‰ heavier than THC.

The expelled *n*-alkanes also become heavier as the temperature increases (Fig. 5(b)). TH380L, TH410L and TH460L identifies *n*-alkanes expelled at 380, 410 and 460 °C, respectively. There is a trend of isotopic values being heavier as temperature increases. The δ^{13}C values of TH460L are nearly 4‰ heavier than those of TH380L. The carbon isotopic compositions of *n*-alkanes from the expelled hydrocarbon fraction are all different from that of the original sample. The δ^{13}C values of TH380L are slightly lighter than

THC, while TH410L and TH460L are both heavier than THC.

There are obvious differences between the δ^{13}C values of *n*-alkanes in unexpelled EOM and in expelled oils (Fig. 5(c)). The δ^{13}C values of TH410C are around 2‰ heavier than TH410L; the δ^{13}C values of TH380C are nearly 4‰ heavier than TH380L. The big differences between the δ^{13}C values of unexpelled EOM and expelled oils show that there is a kinetic isotopic fractionation effect in the hydrocarbons expelled from Tuha desmocollinite. The *n*-alkanes expelled are lighter than *n*-alkanes of the unexpelled EOM. An increase of temperature increases the expulsion efficiency and may decrease the isotopic fractionation effect.

An additional experiment was done to further the understanding of isotopic fractionation associated with expulsion. The 80 mesh Tuha desmocollinite was soxhlet extracted for 72 h to deplete the adsorptive hydrocarbon in it. The extracted desmocollinite was heated for 72 h at 410 °C in the same pyrolysis system. TH410C* identifies *n*-alkanes of unexpelled extracts, TH410L* identifies *n*-alkanes of expelled oil. The δ^{13}C values of TH410C* are 1‰ heavier than TH410L* (Fig. 5(d)).

Table 4
$\delta^{13}C$ values (‰) for *n*-alkanes in pyrolysates (unexpelled and expelled) of S38 at different temperatures

ID	S38-C	S38-350C	S38-380C	S38-410C	S38-350L	S38-380L	S38-410L
10							−25.7
11							−25.5
12						−24.1	−25.5
13						−24.5	−25.3
14					−23.9	−24.6	−25.6
15	−26.2				−24.4	−24.1	−25.5
16	−26.5				−24.5	−24.2	−25.5
17	−26.8	−23.0			−24.6	−24.3	−25.5
18	−27.4	−23.2	−23.0		−24.6	−24.3	−26.0
19	−27.0	−22.6	−22.7		−24.0	−24.4	−26.4
20	−28.0	−22.9	−22.9	−25.9	−24.0	−24.5	−26.4
21	−27.8	−22.7	−22.6	−26.3	−23.7	−24.8	−26.4
22	−27.2	−22.2	−22.9	−26.0	−23.7	−25.4	−26.5
23	−27.0	−22.3	−22.6	−25.5	−23.7	−25.5	−26.2
24	−27.4	−22.1	−22.7	−25.9	−23.8	−25.2	−26.6
25	−26.9	−22.1	−22.9	−25.7		−25.5	−26.7
26	−26.7	−21.9	−22.6	−26.0		−25.9	−26.4
27	−26.9	−22.0	−22.5	−26.6		−26.0	−26.2
28	−26.5	−22.1	−22.8	−26.6		−25.9	
29	−26.5	−22.4	−23.6			−26.0	
30	−26.4	−23.1	−23.9			−25.7	
31	−25.9	−22.8				−25.0	

ID, carbon number of *n*-alkanes.

Table 5
Identifiers for *n*-alkanes (unexpelled and expelled) of ZM at different temperatures

Temperature (°C):	320	350		380		410		460		510	
	EOM	EOM	Expelled	EOM	Expelled	EOM	Expelled	EOM	Expelled	EOM	Expelled
	ZM320C	ZM350C	ZM350L	ZM380C	ZM380L	ZM410C	ZM410L	ZM460C	ZM460L	ZM510C	ZM510L

3.2. Carbon isotopic composition of individual n-alkanes in pyrolysates of Tuha mudstone S38

Usually the $\delta^{13}C$ value of generated oil will gradually become heavier with the increase in maturity. However, with an increase of the pyrolysis temperature, the $\delta^{13}C$ values of generated *n*-alkanes of Tuha mudstone (S38) become depleted in ^{13}C (Fig. 6(a)). The reason is not yet clear and needs to be studied further. S38-C is the original extract from the Tuha mudstone, S38-350C, S38-380C and S38-410C are the *n*-alkanes extracted from the pyrolysis residues at 350, 380 and 410 °C, respectively. The unexpelled EOMs of S38 show a trend of becoming lighter as temperature increases.

The $\delta^{13}C$ values of *n*-alkanes extracted from original S38 are more depleted in ^{13}C compared with *n*-alkanes in unexpelled extracts at 350, 380 and 410 °C (Fig. 6(a)), and also lighter than *n*-alkanes expelled at various temperatures. The expelled oils of S38 also show a trend of becoming lighter as temperature increases (Fig. 6(b)).

The obvious differences between the $\delta^{13}C$ values of unexpelled *n*-alkanes and expelled *n*-alkanes at both

350 and 380 °C are shown in Fig. 6(c). This difference is over 2‰ at 380 °C, a little bigger than the difference at 350 °C. It is smaller than that in the Tuha desmocollinite but still obvious. However the difference at 410 °C is small. Thus, as the expulsion efficiency increases, the isotopic fractionation effect decreases with increasing temperature, which is similar to the situation in Tuha desmocollinite.

3.3. Carbon isotopic composition of individual n-alkanes in pyrolysates of Fushun cannel coal

The $\delta^{13}C$ values of *n*-alkanes of unexpelled hydrocarbons in Fushun cannel become slightly enriched in ^{13}C as the temperatures increase (Fig. 7(a)). There is a 2‰ increment as temperatures increase from 320 to 510 °C. In contrast, the $\delta^{13}C$ values of *n*-alkanes in expelled pyrolysates at each temperature are very close to each other (Fig. 7(b)).

ZM-350C is lighter than ZM-350L. This may be related to the expulsion of early generated hydrocarbons with lighter $\delta^{13}C$ values adsorbed in the original cannel

Table 6
δ^{13}C values (‰) for n-alkanes in pyrolysates (unexpelled and expelled) of Fushun cannel at different temperatures[a]

| ID	ZM320C	ZM350C	ZM380C	ZM410C	ZM460C	ZM510C	ZM350L	ZM380L	ZM410L	ZM460L	ZM510L
10								−30.4	−29.9		−29.1
11							−30.5	−30.3	−29.5	−29.2	−29.6
12							−30.2	−30.4	−29.4	−29.0	−29.5
13							−30.2	−30.7	−30.3	−29.2	−29.5
14		−28.7	−28.7	29.7			−30.1	−30.4	−30.1	−28.9	−29.4
15	−30.8	−30.9	−29.8	−29.6			−30.1	−30.6	−30.4	−29.2	−29.3
16	−30.5	−30.8	−31.1	−29.6	−28.2		−30.8	−30.9	−30.6	−29.9	−29.4
17	−30.5	−30.4	−31.4	−29.4	−28.6	−30.4	−30.6	−31.0	−30.5	−30.1	−29.4
18	−31.0	−31.5	−31.3	−29.1	−28.7	−29.8	−31.0	−31.3	−30.9	−30.4	−30.5
19	−30.6	−32.3	−31.2	−29.4	−29.0	−30.0	−30.9	−31.7	−30.9	−30.5	−30.8
20	−31.0	−32.2	−31.0	−29.2	−28.9	−29.5	−31.5	−31.4	−30.9	−30.4	−30.9
21	−31.7	−32.1	−31.1	−29.6	−29.1	−30.1	−31.0	−31.9	−31.0	−30.8	−30.8
22	−32.1	−32.3	−30.7	−29.8	−29.2	−30.0	−30.7	−31.9	−31.1	−30.6	−30.5
23	−32.4	−32.5	−30.5	−30.0	−29.3	−29.7	−30.8	−32.0	−30.9	−30.8	−30.6
24	−32.5	−32.8	−30.7	−29.9	−29.2	−29.7	−30.7	−32.2	−31.0	−30.7	−30.9
25	−32.4	−32.7	−30.6	−29.8	−29.4	−29.6	−30.4	−31.8	−30.7	−30.7	−31.4
26	−32.7	−32.6	−30.8	−29.3	−29.5	−29.8	−30.4	−32.4	−30.7	−31.0	−31.0
27	−33.0	−32.3	−30.7	−29.6	−29.6	−29.7	−30.6	−31.9	−31.2	−30.6	−30.8
28	−33.2	−32.2	−30.8	−30.3	−29.7	−29.8	−31.1	−32.4	−31.3	−31.0	−30.9
29	−33.4	−32.4	−31.0	−30.9	−30.1		−31.0	−32.4	−31.3	−31.0	−31.1
30	−33.7	−32.9	−31.4	−31.4	−30.0			−32.9	−31.4		−31.1
31	−34.1	−33.0	−31.2	−31.8	−30.1				−31.5		−31.4
32		−33.0									−31.7

[a] ID, carbon number of n-alkanes.
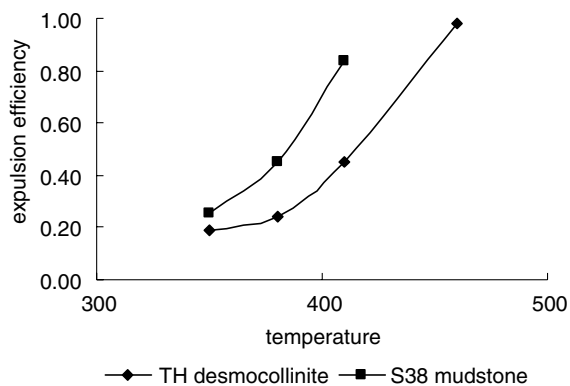
Fig. 4. Expulsion efficiency increases at higher temperature.

sample. The adsorbed hydrocarbons are not completely expelled out of cannel at 350 °C. There is no obvious isotopic fractionation effect between unexpelled n-alkanes and expelled n-alkanes during the expulsion of Fushun cannel (Fig. 7(c)). The differences between the δ^{13}C of unexpelled n-alkanes and expelled n-alkanes are small at every temperature. This suggests that there was almost no isotopic fractionation in the experiment. The work of Xiong et al. (2000) showed a similar result, i.e., no obvious carbon isotopic composition fractiona-

tion during hydrocarbon expulsion in the Liaohe mudstone (Type II kerogen).

Previous studies (Clayton and Bjorøy, 1994) show that maturity accounts for between 50% and 90% of the observed isotopic variation, all values becoming heavier with increasing maturity, typically by between 2‰ and 3‰. The pyrolysis experiments of TH desmocollinite, S38 mudstone and Fushun cannel prove that maturation has a significant effect on the δ^{13}C values of pyrolysis products.

A considerable compositional fractionation of hydrocarbons may occur during migration in laboratory simulation experiments (Bonilla and Engel, 1985). With increased migration distance the δ^{13}C values for the aromatic hydrocarbon fractions remain relatively unchanged, while the aliphatic and NSO fractions become slightly depleted in ^{13}C with increased distance of migration. This fractionation effect might become accentuated with increasing migration distance and should be considered when trying to make oil to oil or oil to source rock correlations. The results also show that isotopic fractionation effects increased as the particle size used in the HPLC simulation experiments decreased. In the HPLC migration experiment there was depletion in ^{13}C ranging up to 2.26‰.

The strong adsorptive capacity of Type III kerogens is responsible for the chromatography-like effect in
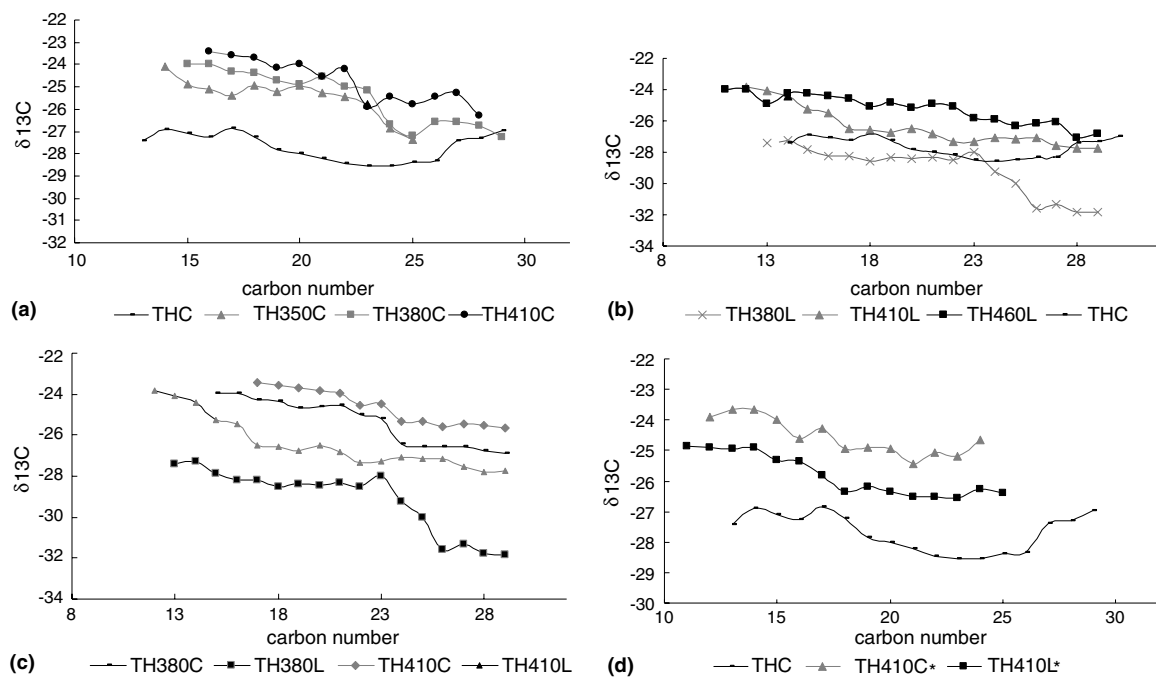
Fig. 5. (a) $\delta^{13}C$ values of n-alkanes in unexpelled extracts of Tuha desmocollinite at different temperatures. (b) $\delta^{13}C$ values of n-alkanes in expelled products of Tuha desmocollinite at different temperatures. (c) $\delta^{13}C$ values of n-alkanes in both unexpelled extracts and expelled hydrocarbons of Tuha desmocollinite at 380 and 410 °C. (d) $\delta^{13}C$ values of n-alkanes in unexpelled extracts and expelled hydrocarbons after heating the pre-extracted Tuha desmocollinite at 410 °C.
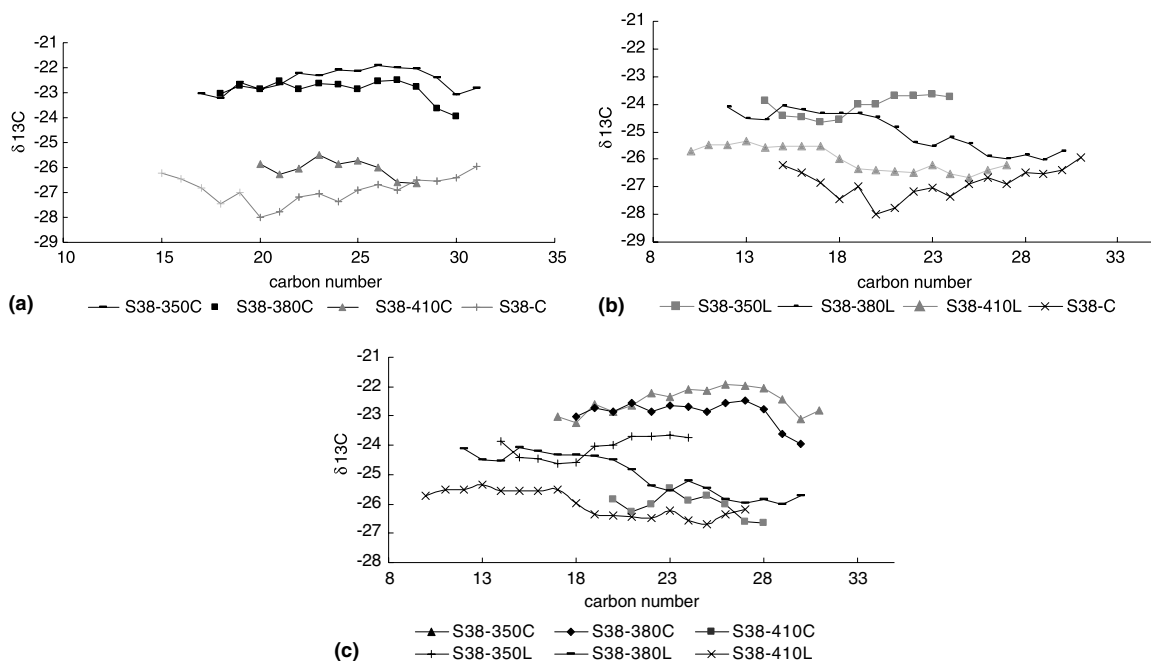
Fig. 6. (a) $\delta^{13}C$ values of n-alkanes in unexpelled pyrolysates of S38 at different temperatures. (b) $\delta^{13}C$ values of n-alkanes in expelled pyrolysates of S38 at different temperatures. (c) $\delta^{13}C$ values of n-alkanes in both unexpelled and expelled hydrocarbons of S38 at different temperatures.
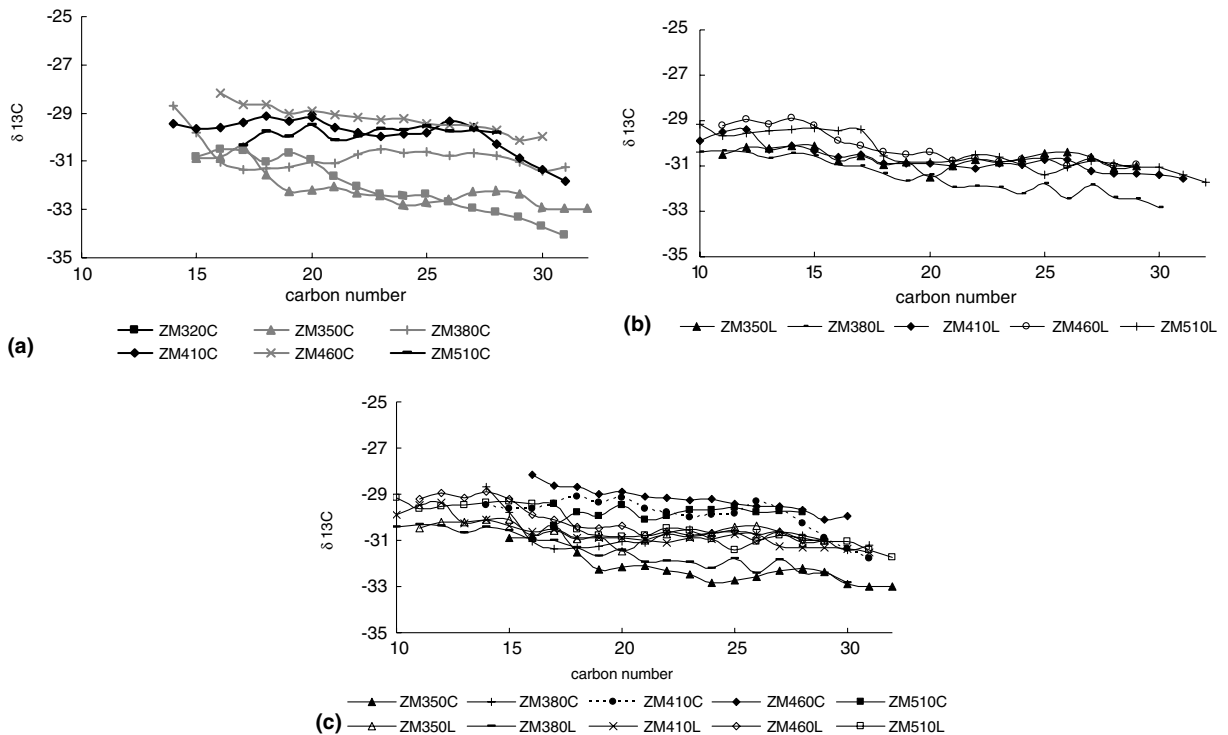
Fig. 7. (a) $\delta^{13}C$ values of *n*-alkanes in unexpelled pyrolysates of cannel at different temperatures. (b) $\delta^{13}C$ values of *n*-alkanes in expelled pyrolysates of cannel at different temperatures. (c) $\delta^{13}C$ values of individual *n*-alkanes from expelled hydrocarbons and unexpelled extracts of cannel at different temperatures.

expulsion. Fractionation of petroleum fractions occurs in this sequence: asphaltenes > polars, resins > aromatics > branched alkanes > *n*-alkanes during this process; the latter being preferentially expelled with respect to the former groups (Pepper and Corvi, 1995). Vitrinite has a high proportion of nano-pores (Parkash and Chakrabartty, 1986). These pores would contribute much to the internal surface area at which adsorption occurs, and may act as sites for capillary condensation and molecular sieving, thus vitrinite shows a very large retention capacity (Ritter, 2003). Vitrinite, desmocollinite and some other Type III source rocks like Tuha mudstone S38 have stronger adsorptive capacity than Type II source rocks such as the Fushun cannel and the Liaohe mudstone. During expulsion hydrocarbons are expelled out by diffusion with or without other carrier. Adsorption and desorption occur on the internal surface throughout hydrocarbon expulsion. Hydrocarbons with heavier $\delta^{13}C$ values may diffuse slowly because they are easier to be adsorbed and harder to be desorbed. For Tuha desmocollinite, *n*-alkanes in unexpelled EOMs are heavier than expelled *n*-alkanes. There is a trend of becoming heavier at higher temperatures for *n*-alkanes in both unexpelled EOMs and expelled hydrocarbons. For S38 mudstone, though *n*-alkanes in both unexpelled

EOMs and expelled hydrocarbons become lighter at higher temperatures, *n*-alkanes in unexpelled EOMs are still heavier than *n*-alkanes expelled. Therefore, the selective adsorption and desorption may be responsible for the isotopic fractionation effect during expulsion in our experiment.

4. Conclusions

The influence of hydrocarbon expulsion on carbon isotopic compositions of individual *n*-alkanes in pyrolysates of some terrestrial kerogens has been experimentally studied. It can be concluded (1) that there is carbon isotopic fractionation during hydrocarbon expulsion from Type III kerogens in Tuha Basin; (2) that there is almost no carbon isotopic fractionation during hydrocarbon expulsion from Type II kerogens in Fushun and Liaohe basin; (3) that carbon isotopic fractionation during hydrocarbon expulsion should be considered in making oil-source correlation of Type III kerogens in the Tuha Basin; (4) that oil and source at different maturities cannot be correlated directly, pyrolysates with low maturity are usually depleted in ^{13}C; and (5) that for Type III kerogens the carbon isotopic

compositions of expelled hydrocarbons are usually lighter than the hydrocarbons remaining in the source rocks because of strong adsorptive capacity.

Acknowledgement

References

Bjorøy, M., Hall, K., Gillyon, P., Jumeau, J., 1991. Carbon isotope variations in *n*-alkanes and isoprenoids of whole oils. Chemical Geology 93, 13–20.

Bjorøy, M., Hall, K., Moe, R.P., 1994. Stable carbon isotope variations in *n*-alkanes in Central Graben oils. Organic Geochemistry 22, 355–381.

Bonilla, J.V., Engel, M.H., 1985. Chemical and isotopic redistribution of hydrocarbons during migration: laboratory simulation experiments. Organic Geochemistry 10, 181–190.

Clayton, C.J., Bjorøy, M., 1994. Effect of maturity on $^{13}C/^{12}C$ ratios of individual compounds in North Sea oils. Organic Geochemistry 21, 737–750.

Ellis, L., Fincannon, A.L., 1998. Analytical improvements in irm–GC/MS analyses: advanced techniques in tube furnace design and sample preparation. Organic Geochemistry 29 (5–7), 1101–1117.

Freeman, K.H., Hayes, J.M., Trendel, J.M., Albrecht, P., 1990. Evidence from carbon isotope measurements from diverse origins of sedimentary hydrocarbons. Nature 343, 254–256.

Geng, Ansong, Zhou, Yi, Fu, Jiamo, Sheng, Guoying, Zhang, Qiming, 1998. The generation and expulsion of gases in Ya131 gas field, South China Sea: implication of laboratory pyrolysis results. Journal of Asian Earth Sciences 16 (4), 429–436.

Hayes, J.M., Freeman, K.H., Popp, B.N., Hoham, C.H., 1990. Compound-specific isotopic analyses: a novel tool for reconstruction of ancient biochemical processes. Organic Geochemistry 16, 1115–1128.

Hendrix, M.S., Brassel, S.C., Carroll, A.R., Graham, S.A., 1995. Sedimentology, organic geochemistry, and petroleum potential of Jurassic coal measures: Tarim, Junggar, and Turpan basins, Northwest China. AAPG Bulletin 79, 929–959.

Huang, D., Zhang, D., Li, J., Huang, X., 1991. Hydrocarbon genesis of Jurassic coal measures in the Turpan basin, China. Organic Geochemistry 17, 827–838.

Karlsen, D.A., Nyland, B., Flood, B., Ohm, S.E., Brekke, T., Olsen, S., Backer-Owe, K., 1995. Petroleum Geochemistry of the Haltenbanken, Norwegian Continantal Shelf. In: Cubbit, J.M., England, W.A. (Eds.), The Geochemistry of Reservoirs Geological Society, 86. Special Publication, London, pp. 203–254.

Leythaeuser, D., Radke, M., Schaefer, R.G., 1984. Efficiency of petroleum expulsion from shale source rocks. Nature, London 311, 745–748.

Parkash, S., Chakrabartty, S.K., 1986. Microporosity in Alberta Plains coals. Journal of Coal Geology 6, 55–70.

Pepper, A.S., Corvi, P.J., 1995. Simple kinetic models of petroleum formation. Part III: modelling an open system. Marine and Petroleum Geology 12, 417–452.

Rieley, G., Collier, R.J., Jones, D.M., Eglinton, G., Eakin, A.E., Fallick, A.E., 1991. Sources of sedimentary lipids deduced from stable carbon-isotope analyses of individual compounds. Nature 352, 425–427.

Ritter, U., 2003. Solubility of petroleum compounds in kerogen: implications for petroleum expulsion. Organic Geochemistry 34, 319–326.

Ruble, T.E., Bakel, A.J., Philp, R.P., 1994. Compound specific isotopic variability in Uinta Basin native bitumens: paleoenvironmental implications. Organic Geochemistry 21, 661–671.

Schoell, M., Schouten, S., Sinninghe Damste, J.S., de Leeuw, R.E., Summons, R.E., 1994. A molecular organic carbon isotope record of Miocene climate changes. Science 263, 1122–1125.

Stoddart, D.P., Hall, P.B., Larter, S.R., Brasher, J., Maowen, Li, Bjorøy, M., 1995. The reservoir geochemistry of the Eldfish Field, Norweigian North Sea. In: Cubitt, J.M., England, W.A. (Eds.), The Geochemistry of Reservoirs Geological Society, 86. Special Publication, London, pp. 257–279.

Sun, Yongge, Guoying, Sheng, Ping'an, Peng, Jiamo, Fu, 2000. Compound-specific stable carbon isotope analysis as a tool for correlating coal-sourced oils and interbedded shale-sourced oils in coal measures: an example from Turpan basin, north-western China. Organic Geochemistry 31, 1349–1362.

Van Krevelen, D.W., 1961. Coal Typology-Chemistry-Physics-Constitution. Elsevier, Amsterdam 514pp.

Xiong, Yongqiang, Ansong, Geng, Chunjiang, Wang, Guoying, Sheng, Jiamo, Fu, 2003. The origin of crude oils from the Shuguang-Huanxiling buried Hills in the Liaohe Basin, China: evidence from chemical and isotopic compositions. Applied Geochemistry 18, 445–456.

Xiong, Yongqiang, Ansong, Geng, 2000. Carbon isotopic composition of individual *n*-alkanes in asphaltene pyrolysates of biodegraded crude oils from the Liaohe Basin, China. Organic Geochemistry 31, 1441–1449.

Zhang, X., 1997. Carbon isotopic geochemistry of coal-generated hydrocarbons in Turpan Basin, North-western, China. Ph.D. Thesis, Lanzhou Institute of Geology, Chinese Academy of Sciences.